

SCIENTIFIC REPORTS



OPEN

Precise Control of the Number of Layers of Graphene by Picosecond Laser Thinning

Received: 19 February 2015

Accepted: 22 May 2015

Published: 26 June 2015

Zhe Lin¹, Xiaohui Ye¹, Jinpeng Han¹, Qiao Chen^{1,2}, Peixun Fan¹, Hongjun Zhang¹, Dan Xie³, Hongwei Zhu^{1,2} & Minlin Zhong¹

The properties of graphene can vary as a function of the number of layers (NOL). Controlling the NOL in large area graphene is still challenging. In this work, we demonstrate a picosecond (ps) laser thinning removal of graphene layers from multi-layered graphene to obtain desired NOL when appropriate pulse threshold energy is adopted. The thinning process is conducted in atmosphere without any coating and it is applicable for graphene films on arbitrary substrates. This method provides many advantages such as one-step process, non-contact operation, substrate and environment-friendly, and patternable, which will enable its potential applications in the manufacturing of graphene-based electronic devices.

Graphene, a one-atom thick layer of graphite with densely packed sp²-bonded carbon atoms¹, has been extensively investigated since its first production/generation in the lab by Geim, *et al.*² in 2004. The unique properties such as electron mobility of $2.5 \times 10^5 \text{ cm}^2 \text{ V}^{-1} \text{ s}^{-1}$ at room temperature³, high thermal conductivity ($> 3000 \text{ W m K}^{-1}$)^{4,5} and optical absorption of exactly $\pi\alpha = 2.3\%$ have been reported⁶. Depending on these properties, graphene is considered to be the next-generation materials of transistors, transparent conductive electrodes and in other applications⁷. The properties of graphene, such as electronic structure and optical transparency are functions of its number of layers (NOL)^{8,9}. Therefore, it is significantly important to accurately control the number of graphene layers. Although many groups have reported the synthesizing of monolayer or bilayer graphene, to control the NOL in graphene synthesis is still challenging¹⁰. Thus, the post-treatment of few-layer graphene to achieve the accurate control of the NOL is an alternative approach.

There are several studies which reported the top-down methods that used some methods reducing graphene thickness to achieve the specific number of layers. Huang, *et al.*¹¹ reported an *in-situ* sublimation of the suspended graphene inside transmission electron microscopy (TEM). Graphene was peeled layer-by-layer using Joule heating to induce the atom sublimation and electron beam irradiation to facilitate the atom displacement. Yang, *et al.*⁷ proposed a simple and efficient method of thinning graphene by mild nitrogen plasma irradiation and annealing in Ar/O₂. Nitrogen plasma attacked the top-layer plane, introducing defects into the lattice; oxygen molecules etched out the carbon atoms at the edge of defect sites, finally removing the damaged top layer. All other top-down methods also included inducing the defects on the top layers of graphene through oxidation or plasma treatments^{7,12}. Han, *et al.*¹³ proposed a method of producing monolayer graphene by laser irradiation. The upper layers of graphene were selectively oxidized under the laser heating; and the bottom monolayers of graphene were kept well because the substrates played as a heat sink and absorbed the extra energy. Dimiev, *et al.*⁸ demonstrated a novel approach of layer-by-layer removal of graphene. A Zn layer was first coated on the few-layer graphene by sputtering. Then Zn was dissolved in diluted acid, meanwhile, the acid removed the damaged graphene

¹School of Materials Science and Engineering, Tsinghua University, Beijing 100084, China. ²State Key Laboratory of New Ceramics and Fine Processing, Tsinghua University, Beijing 100084, China. ³Tsinghua National Laboratory for Information Science and Technology (TNList), Institute of Microelectronics, Tsinghua University, Beijing 100084, China. Correspondence and requests for materials should be addressed to M.Z. (email: zhml@tsinghua.edu.cn) or H.Z. (email: hongweizhu@tsinghua.edu.cn)

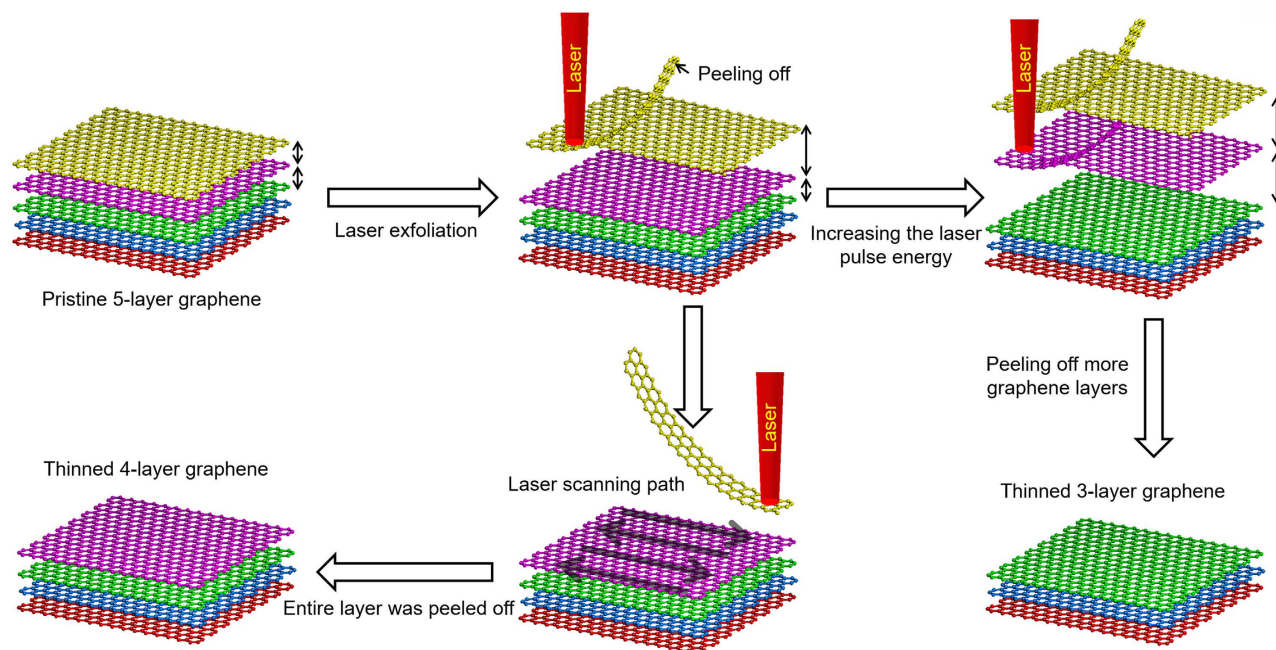


Figure 1. Schematics of laser thinning process.

top layers. All of the methods mentioned above showed the capability of thinning graphene, and some had a good potential in accurately controlling the number of graphene layers. However, it is obvious that all these methods have some kinds of limitations. The layer-by-layer thinning method includes making defects on the graphene top layers and removing the damaged layers, followed by a multiple-step process, which requires more equipment and strict reaction/processing conditions. Furthermore, these methods can only remove one graphene layer in one process, which represents that if a few layers of graphene are needed to be removed, the process needs to be repeated several times. On the other hand, the one-step methods can only thin the graphene to monolayer or bilayer, which cannot reach the purpose of preparing electronics with different properties by controlling the number of graphene layers.

Laser has been employed in graphene treatments, including direct laser writing, laser patterning and laser induced synthesis. For examples, EI-Kady, *et al.*¹⁴ reported a graphene-based electrochemical capacitor with reduced graphene oxide electrodes obtained using a standard light-scribe DVD laser. Kalita, *et al.*¹⁵ proposed a method for micropatterning of graphene by femtosecond laser. Park, *et al.*¹⁶ demonstrated a rapid single-step fabrication of graphene patterns using laser assisted chemical vapor deposition (LCVD).

Here, a novel yet simple method of picosecond (ps) laser thinning is proposed to accurately control the number of graphene layers. The graphene films can be thinned to the specific number of layers using the scanning laser radiation with tunable pulse threshold energy in atmospheric condition. In the process, arbitrary patterns are achievable if the unique scanning paths are set up. Because this process/method has many advantages, such as one-step process, non-contact operation, substrate and environmental-friendly, and patternable thinning, it will be potentially used in the fabrication of graphene-based electronic devices.

Results

Laser Thinning. The ps laser thinning process of graphene is demonstrated in Fig. 1. The laser irradiated on the pristine graphene sample (5-layer), causing the increasing of the distance between the top layer and the bottom layers. Then the graphene within the laser irradiation area was peeled off. The whole layer was peeled off by the laser beam scanning and the graphene sample was thinned to 4-layer. Furthermore, by increasing the laser pulse energy, more top layers were lifted up and peeled off from bottom, to obtain graphene film with less number of layers. Therefore, the number of graphene layers can be precisely controlled by adjusting the laser pulse energy.

Figure 2a shows the photographs of graphene transferred on the transparent substrate, *e.g.* poly(dimethylsiloxane)(PDMS). The pristine (5-layer) to monolayer graphene are displayed from left to right. A typical optical image of graphene with different layer numbers is shown in Fig. 2b. The contrast with graphene and substrate (SiO_2/Si) indicates the number of layers, which is further confirmed by Raman (Fig. 2c–g), visible transmission spectra (Fig. 2h) and Atomic Force Microscopy (AFM) image of graphene (Fig. 2i).

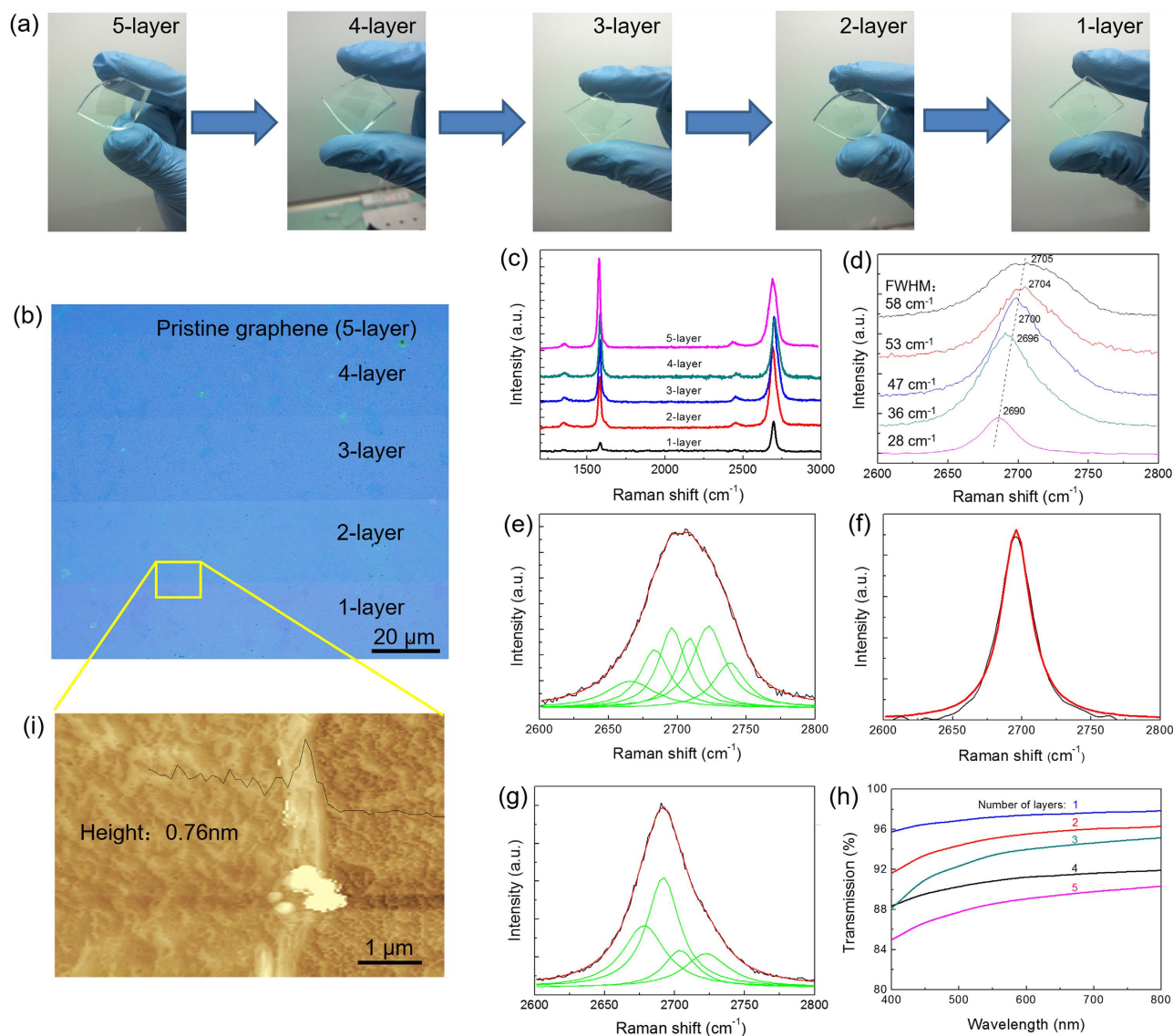


Figure 2. (a) Photographs and (b) optical image of graphene with different NOL obtained by laser thinning. (c) Raman spectra of graphene with different numbers of layers. (d) Corresponding 2D peak position and FWHM. The splitting of 2D peak by Lorentzian fitting: (e) 5-layer, (f) monolayer and (g) bilayer graphene. (h) Transmittance spectra. (i) AFM image.

Raman is a powerful tool to determine the number of graphene layers and evaluate their qualities⁷. The two intense peaks located at $\sim 1580\text{ cm}^{-1}$ and $\sim 2700\text{ cm}^{-1}$ represent the characteristic G peak and 2D peak. The peak intensity ratio of G to 2D (I_G/I_{2D}) reflects the number of graphene layers. The position, full width at half maximum (FWHM), and Lorentzian fitting of 2D peak supply further evidences for determining the layer number of graphene¹⁵. Raman spectra in Fig. 2c were recorded from the samples as shown in Fig. 2b from top to bottom. The decrease of I_G/I_{2D} from 1.3 to 0.3 (Fig. 2c) reveals the reduction of graphene layers from 5 to 1. In Fig. 2d, the position of 2D peak shows blue-shifts from 2705 cm^{-1} (5-layer) to 2690 cm^{-1} (1-layer) and the FWHM (2D) decreases from 58 cm^{-1} (5-layer) to 28 cm^{-1} (1-layer), which is consistent with the result that the 2D peak position blue-shift following the layer decrease¹⁵. For a multilayer graphene, the 2D peak is asymmetric and composed of multiple sub-peaks, as shown in Fig. 2e. However, upon laser thinning, the monolayer graphene shows a symmetric 2D peak, which is fitted by only one sub-peak (Fig. 2f). Meanwhile, the bilayer graphene has a symmetric 2D peak and can be fitted by four sub-peaks (Fig. 2g). All these results indicate that the graphene film is indeed thinned through the laser thinning process.

To accurately determine the number of graphene layers, the visible transmittances of graphene samples were measured. The optical image shows that the graphene films are uniform after the same laser thinning process, and the transmittance of graphene monotonically decreases following the layer increase

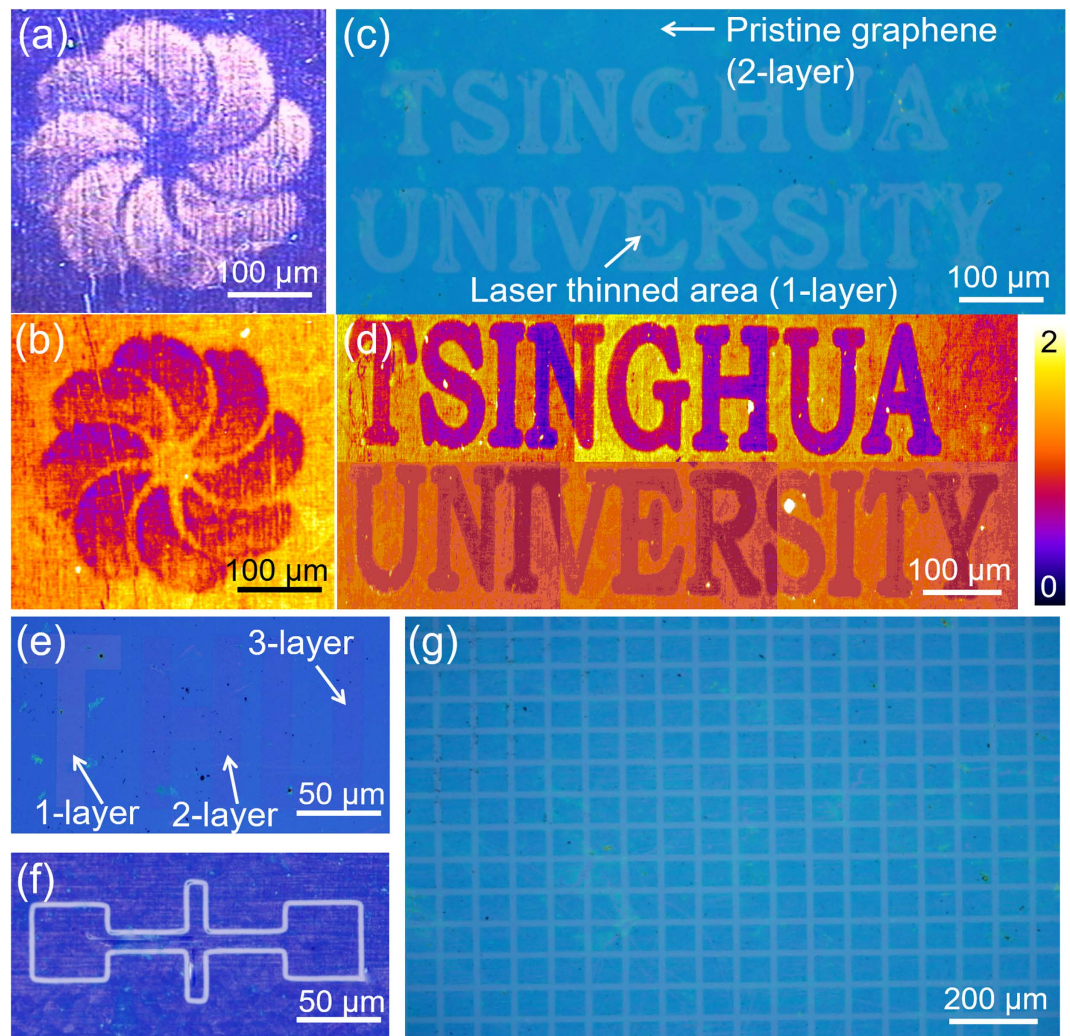


Figure 3. (a) Optical image and (b) Raman mapping image of a windmill pattern. (c) Optical image and (d) Raman mapping image of the word pattern “TSINGHUA UNIVERSITY”. (e) Optical contrast of graphene layers obtained with different laser thinning parameters. The letter “T” represents the monolayer, “H” bilayer, and “U” tri-layer graphene. (f) FET-like and (g) mesh-like patterns of graphene.

of graphene. As shown in Fig. 2h, the transmittance of monolayer graphene is 97.22%, which is well fitted with the theoretical value¹ of the optical absorption (2.3%) for monolayer graphene. With the layers increasing one by one, the transmittance decreases correspondingly from 97.22% to 88.60%, and the pristine graphene with 5 layers has the lowest transmittance. Further, the AFM image in Fig. 2i correlates the position of the yellow box in Fig. 2b. The relative height difference between the bilayer and monolayer is 0.76 nm, which is conformed to the height of 1-layer graphene prepared by CVD method⁸. Therefore, pristine graphene films of 5-layer are thinned by the laser to 4-layer, 3-layer, bilayer and monolayer graphene, separately. The resistance of pristine graphene was about 200 Ω , which was increased to about 500 Ω when the number of layers number was reduced to 1. It is worth noting that the oxidation and doping could influence the surface resistance. Raman spectra of both thinned areas and peeled-off pieces showed that there were few oxidation sites present. Therefore, we considered the change of surface resistance was mainly affected by the number of layers of graphene.

Laser Patterning. The results reported above demonstrate that the one-step laser processing method can produce the graphene with accurate NOL. On the other hand, since graphene-based materials are considered as the promising alternatives to silicon-based ones in the future electronic devices, the patterning of graphene is an essential step in microelectronic processing¹⁷. Figure 3a shows a windmill pattern produced by laser on graphene sample, in which the windmill area is monolayer graphene and the pristine area is 5-layer. The result is confirmed by the Raman mapping image recorded at the same area (Fig. 3b). The contrast in the Raman image indicates the different ratios of I_G/I_{2D} . The purple area represents the lowest I_G/I_{2D} ratio, which indicates the presence of monolayer graphene. The yellow area

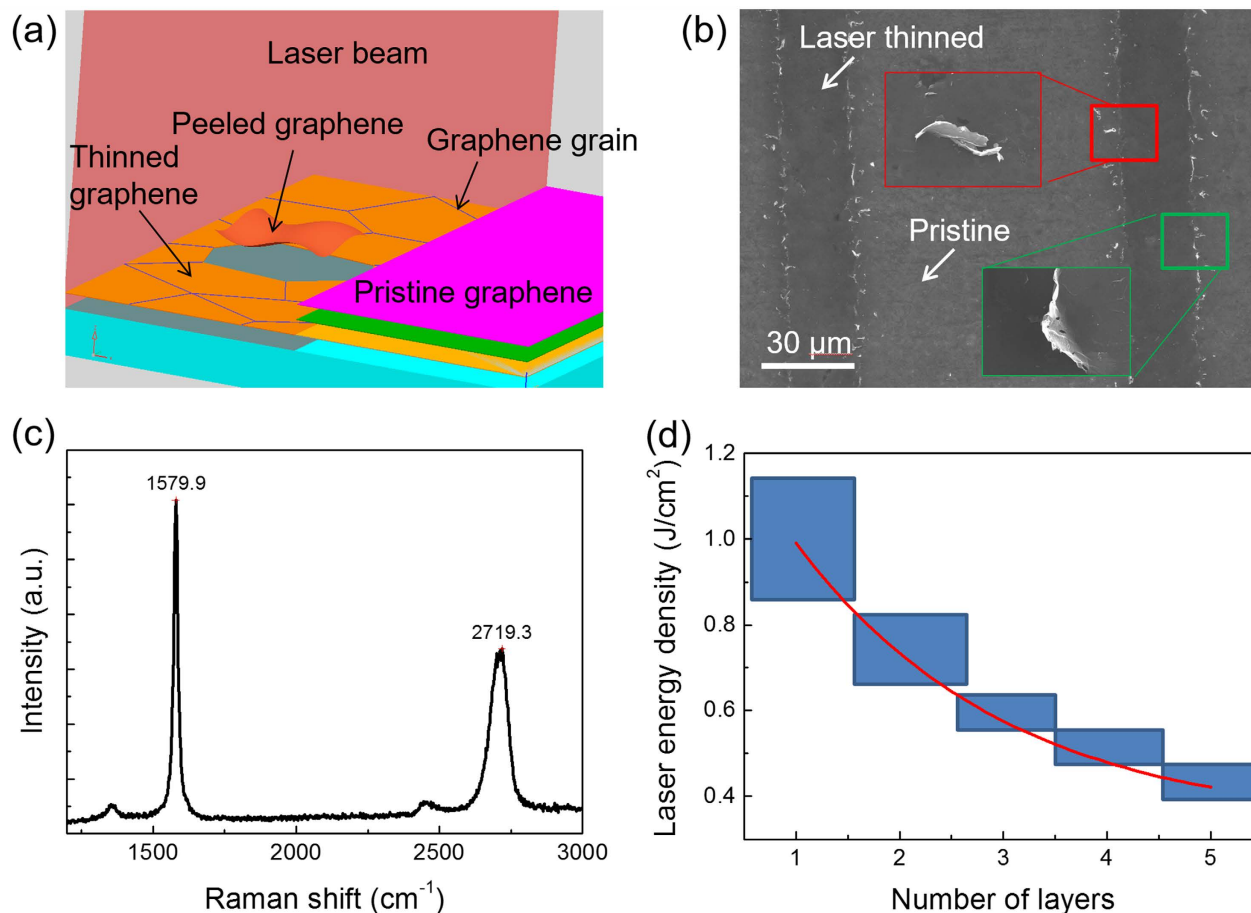


Figure 4. (a) Schematics for the mechanism of laser thinning. (b) SEM image and (c) Raman spectrum of the graphene sample after laser peeling off. (d) Thresholds of the laser energy density to obtain graphene with different NOL.

represents the 5-layer graphene. The word “TSINGHUA UNIVERSITY” with monolayer graphene is patterned on a bilayer graphene sample (Fig. 3c) and the Raman image from the same area is shown in Fig. 3d. The background ratio of I_G/I_{2D} is about 1, which points out that the pristine graphene is bi-layered. After the laser processing, the letter area is thinned to monolayer, which is determined by the I_G/I_{2D} ratio reduced to 0.5. Using different laser energy density, graphene samples with different NOL are obtained. The areas of letter T, H and U are monolayer, bilayer and 3-layer graphene, respectively.

Discussion

Mechanism. The mechanism of the one-step laser thinning process is further proposed. Figure 4a shows the schematic of the “peeling off” mechanism of graphene thinning. The D peak at $\sim 1350\text{ cm}^{-1}$ represents the signal from defects and impurities, and the ratio of D peak and G peak (I_D/I_G) is widely applied to characterize the crystallization quality of graphene¹⁸. Figure 2c reveals that the I_D/I_G keeps fairly low during all the thinning process, which is different from the layer-by-layer methods⁶. The low D peak indicates that there is no oxidation during the thinning process. The photon energy of the laser used in this process was 1.2 eV (1064 nm laser), which was much lower than the formation energy of C-C bond in ideal graphene (3.7 eV). The laser couldn’t directly break the C-C bond and sublimate the graphene. However, the graphene samples used in our experiments were grown using CVD method, and the graphene layers were composed of grains containing crystalline defects. The bonds on the grain boundaries with defects were much weaker than the defect-free C-C bonds. These defect bonds could be easily broken by the laser photons. The Van der Waals force, which attracted the neighboring graphene layers together, was 0.17 eV, much smaller than the photon energy of the laser. In the interaction of the photon and graphene, the distance of the interacting grains and their adjacent layers increased¹⁷, the Van der Waals force was weakened further, and finally the grains lost the connection with adjacent grains and were peeled off from underlying graphene layers.

Scanning electron microscope (SEM) was utilized to prove this layer thinning mechanism. Figure 4b shows the SEM image of the laser thinned and pristine areas. To obtain more details about the peeling

off mechanism, the thinning process was conducted at a higher scanning speed (200 mm/s). The residues at the scanning boundary were acquired which did not exist under the optimized scanning parameters. The curls of graphene emerged on the scanning boundaries, *i.e.*, graphene grain residues which were not being completely peeled off (marked with the green box in Fig. 4b). However, the graphene grains in the middle area of the scanning were completely peeled off. Most of grains peeled off by laser disappeared in the air, while some pieces of graphene grains fell onto the graphene near the scanning boundaries (marked with the red box in Fig. 4b). The grain size was about 1 μm , which was much smaller than the laser spot diameter. The graphene sample after being peeled off (Fig. 4b) was characterized by Raman (Fig. 4c). The I_G/I_{2D} is about 2, much higher than the pristine graphene, which indicates the graphene in this area is deformed. It is worth noting that the graphene after being peeled off still has a quite low D peak, which further proves that no oxidation occurs in this process.

The threshold of the laser energy density to thin graphene into specific layers is summarized in Fig. 4d. To obtain monolayer graphene from pristine 5-layer graphene, the threshold of the laser energy density should be up to 1.0 J/cm², which is much higher than the threshold for obtaining a 4-layer graphene (0.5 J/cm²). Dhar, *et al.*¹⁹ studied the relationship of the ablation threshold energy and the numbers of remaining graphene layers. The ablation threshold decreased dramatically following the increase of obtained graphene layers. These phenomena were explained by the different optical absorption coefficients and specific heat of graphene with different layers. This theory explained why laser photons with different energy density could peel off different graphene layers within one process. For example, to get 4-layer graphene, the specific energy density of applied laser photons was higher than the ablation threshold of 4-layer graphene, but lower than that of 3-layer graphene. So only the top layer was peeled off, and the second top-layer was retained. The window of the two adjacent ablation thresholds is the applied energy range in the laser thinning to obtain the graphene with specific layers. This makes obtaining graphene with specific number of layers in one step is achievable. These thresholds were obtained when the grain size of graphene is about 1 μm . Based on the peeling off mechanism proposed above, it can be predicted that the threshold energy will increase with the grain size.

Devices. Due to the unique thickness-dependent electronic properties, high flexibility, and transparency, graphene and its relatives are fantastic materials for both electron active channels and electrodes in various electronic devices²⁰. Graphene with different NOL have different electronic properties. To demonstrate this, field-effect transistors (FETs) were fabricated, as shown in Fig. S1. First, pristine graphene was transferred onto a silicon substrate with 90 nm SiO₂. Then, graphene was thinned to the accurate NOL by laser thinning. As the channel materials and the electrodes, graphene was patterned by lithography, which is displayed in the top-right inset of Fig. S1. The field-effect characteristics with different layer graphene were tested. The mobility of monolayer graphene FET is about 1.4 times of that for bilayer graphene FET. When the NOL is increasing up to 5, the mobility significantly drops to only 130 cm²/Vs. Nagashio, *et al.*^{21,22} reported that with decreasing NOL, the current modulation was enhanced because of the reduction of the interlayer scattering. On the other hand, when the NOL decreased from the bilayer to monolayer, the mobility drastically increased due to the inherent change from the quadric to linear dispersion. While with the increase in NOL, the mobility decreased slightly because of the interlayer scattering. Our result is consistent with the theory, which further confirms that the laser thinning method can accurately control the number of graphene layers.

Conclusion

To conclude, a one-step laser thinning process, with features of non-contact operation, substrate and environment-friendly and patternable, is demonstrated to obtain the accurate number of graphene layers. A “peeling off” mechanism of the laser process is proposed. The thinning process is conducted in atmosphere without any coating. Besides, the laser scanning is applicable for graphene films on arbitrary substrates. All of these advantages make this method have broad potential applications in graphene-based electronic devices.

Experimental Section

Preparation and laser treatment of graphene. Pristine graphene samples were prepared by CVD on copper substrates. The numbers of layers of as-prepared graphene films were confirmed to be 5 by optical microscopy, Raman spectroscopy and optical absorption. Graphene films were then transferred onto Si/SiO₂ substrates¹. The laser using in this work was in picosecond scale with the power of 100 W, and the frequency of 2 MHz. The pattern setup was controlled by a galvanometer, which made the laser beam moving as sited on an objective and with a focus spot of 30 μm . The scanning speed of laser was 100 mm/s, corresponding to a trimming speed of 180 mm²/min. The whole process was conducted in the air ambient.

Characterizations. The optical images were taken using a Nikon microscope. SEM images were obtained using a LEO-1530 microscope (LEO Electron Microscopy. GERMANY). Raman spectra were collected with a HORIBA Lab RAM HR spectrometer (514 nm laser excitation) (HORIBA Jobin Yvon. FRANCE). Raman mapping images were recorded by a Raman 11 spectroscopy (Nanophonon. JAPAN).

AFM images were acquired by a SPM-960 instrument (SHIMADZU, JAPAN). The transmission spectra of graphene were obtained with a UV-visible spectrophotometer.

References

- Li, X. *et al.* Transfer of Large-Area Graphene Films for High-Performance Transparent Conductive Electrodes. *Nano Lett* **9** 4359 (2009).
- Novoselov, K. S. *et al.* Electric field effect in atomically thin carbon films. *Science* **306**, 666 (2004).
- Mayorov, A. S. *et al.* Micrometer-Scale Ballistic Transport in Encapsulated Graphene at Room Temperature. *Nano Lett* **11**, 2396 (2011).
- Balandin, A. A. Thermal properties of graphene and nanostructured carbon materials. *Nature Materials* **10**, 569 (2011).
- Chen, S. *et al.* Thermal conductivity measurements of suspended graphene with and without wrinkles by micro-Raman mapping. *Nanotechnology* **23**, 365701 (2012).
- Nair, R. R. *et al.* Fine structure constant defines visual transparency of graphene. *Science* **320**, 1308 (2008).
- Yang, X. *et al.* Layer-by-layer thinning of graphene by plasma irradiation and post-annealing. *Nanotechnology* **23**, 025704 (2012).
- Dimiev, A. Layer-by-layer removal of graphene for device patterning. *Science* **331**, 1168 (2011).
- Castro Neto, A. H., Guinea, F., Peres, N. M. R., Novoselov, K. S. & Geim, A. K. The electronic properties of graphene. *Rev Mod Phys* **81**, 109 (2009).
- Novoselov, K. S. *et al.* A roadmap for graphene. *Nature* **490**, 192 (2012).
- Huang, J. Y., Qi, L. & Li, J. *In Situ* Imaging of Layer-by-Layer Sublimation of Suspended Graphene. *Nano Research* **3**, 43 (2010).
- Zhao, G., Shao, D., Chen, C. & Wang, X. Synthesis of few-layered graphene by H₂O₂ plasma etching of graphite. *Appl Phys Lett* **98**, 183114 (2011).
- Han, G. H. *et al.* Laser Thinning for Monolayer Graphene Formation: Heat Sink and Interference Effect. *ACS Nano* **5**, 263 (2011).
- El-Kady, M. F., Strong, V., Dubin, S. & Kaner, R. B. Laser Scribing of High-Performance and Flexible Graphene-Based Electrochemical Capacitors. *Science* **335**, 1326 (2012).
- Kalita, G., Qi, L., Namba, Y., Wakita, K. & Umeno, M. Femtosecond laser induced micropatterning of graphene film. *Mater Lett* **65**, 1569 (2011).
- Park, J. B. *et al.* Fast growth of graphene patterns by laser direct writing. *Appl Phys Lett* **98**, 123109 (2011).
- Miyamoto, Y., Zhang, H. & Tomanek, D. Photoexfoliation of Graphene from Graphite: An Ab Initio Study. *Phys Rev Lett* **104**, 208302 (2010).
- Ferrari, A. C. *et al.* Raman spectrum of graphene and graphene layers. *Phys Rev Lett* **97**, 187401 (2006).
- Dhar, S. *et al.* A new route to graphene layers by selective laser ablation. *AIP Adv* **1**, 022109 (2011).
- He, Q. *et al.* Transparent, Flexible, All-Reduced Graphene Oxide Thin Film Transistors. *ACS Nano* **5**, 5038 (2011).
- Nagashio, K., Nishimura, T., Kita, K. & Toriumi, A. Mobility Variations in Mono- and Multi-Layer Graphene Films. *Appl Phys Express* **2**, 025003 (2009).
- Jones, J. D., Shah, R. K., Verbeck, G. F. & Perez, J. M. The Removal of Single Layers from Multi-layer Graphene by Low-Energy Electron Stimulation. *Small* **8**, 1066 (2012).

Acknowledgements

This work was supported by National Program on Key Basic Research Project (2011CB013000), National Science Foundation of China (51210009, 51372133) and Tsinghua National Laboratory for Information Science and Technology (TNList) Cross-discipline Foundation.

Author Contributions

M.L.Z. planned and supervised the project, Z.L. performed the laser experiments with the assistance from X.H.Y., J.P.H., P.X.F. and H.J.Z., Q.C. prepared the graphene samples, D.X. conducted the FET measurement. Z.L., M.L.Z. and H.W.Z. co-wrote the manuscript. All authors discussed and commented on the manuscript.

Additional Information

Supplementary information accompanies this paper at <http://www.nature.com/srep>

Competing financial interests: The authors declare no competing financial interests.

How to cite this article: Lin, Z. *et al.* Precise Control of the Number of Layers of Graphene by Picosecond Laser Thinning. *Sci. Rep.* **5**, 11662; doi: 10.1038/srep11662 (2015).



This work is licensed under a Creative Commons Attribution 4.0 International License. The images or other third party material in this article are included in the article's Creative Commons license, unless indicated otherwise in the credit line; if the material is not included under the Creative Commons license, users will need to obtain permission from the license holder to reproduce the material. To view a copy of this license, visit <http://creativecommons.org/licenses/by/4.0/>